DERIVING REGIONAL SCALE FOREST STRUCTURAL VARIABLES USING EO-1 HYPERION DATA IN COMBINATION WITH AN INVERTED GEOMETRIC-OPTICAL MODEL

Yuan Zeng [a, b, *], Michael E. Schaepman [a], Bingfang Wu [b], Jan G.P.W. Clevers [a], Arnold K. Bregt [a]

[a] Centre for Geo-Information, Wageningen University and Research Centre, the Netherlands - (yuan.zeng, michael.schaepman, jan.clevers, arnold.bregt)@wur.nl
[b] Institute of Remote Sensing Applications, Chinese Academy of Sciences, China – (yuanz, wubf)@irsa.ac.cn

KEY WORDS: EO-1 Hyperion, Forest structural variable, Geometric-optical model, linear spectral unmixing, Three Gorges

ABSTRACT:

The potential of EO-1 Hyperion data combined with an inverted geometric-optical model for the retrieval of forest structural variables in the Longmenhe broadleaved forest natural reserve, located in the Three Gorges region (China), is studied in this paper. Based on the principle of Li-Strahler geometric-optical model, we retrieve the per-pixel reflectance as being a linear combination of four scene components (sunlit canopy/sunlit background and shaded canopy/shaded background). The fraction of each component is subsequently related to several forest structural attributes. With the advantage of having hyperspectral data, we use linear spectral unmixing to separate the above classes present in an atmospherically corrected Hyperion image with support of extensive in situ measurements. In addition, we include DEM derived parameters (slope and aspect) and measured canopy structural parameters for different forest communities to invert the geometric-optical model and retrieve the pixel-based variables forest crown closure (CC) and crown diameter (CD). In total 30 sample plots collected in the Longmenhe study region are used for validation, and the results of the above parameters show a good agreement (e.g., R^2_{CC}=0.64 / RMSE=0.058; R^2_{CD} =0.54 / RMSE=0.71).

1. INTRODUCTION

Human transformations of ecosystems and landscapes are currently one of the largest sources of change on Earth. In particular the provision of ecosystem services, directly affecting human well-being, demand sustainable development and optimal management of natural resources in the coupled human-environment system (GLP, 2005). Population change, land management decisions and practices – amongst others – affect ecosystem properties and therefore require a sustainable socio-economic development in any region on Earth (Murai, 1991). Among the various natural resources that are present on the terrestrial Earth surface, forests are one of the most important contributors that influence ecosystems with respect to carbon storage and release (Schimel et al., 2001). Accurate and up-to-date information on forest structure is essential for many aspects of forest management and changes in forest structure also provide insights related to forest vigor, harvesting, burning, stocking levels, disease, and insect infestations (Wulder, 1998). Thus, quantitatively monitoring forest structure using remote sensing methods strongly supports the conservation and management strategies that take into account biodiversity and the impact of the global carbon cycle.

Main forest structural variables include crown cover, crown size, stem density, tree height, diameter at breast height (DBH), age, spatial distribution, and gap presence etc. Traditionally, quantitative retrieval methods for estimating these variables are grouped into two major categories: statistical and physical approaches. Statistical methods are based mainly on a wide variety of vegetation indices or correlating features and use regression models to infer structural variables directly. Physical methods usually rely on inverting or assimilating canopy reflectance models (Liang, 2004). An observed trend is that more and more empirical, statistical models are being gradually replaced by physically based models.

Canopy reflectance models have been used to improve mapping of many forest structural variables, particularly geometric-optical models, which regard canopy reflectance as a mixture of discrete canopy components (Ustin, 2004). For example, Hall et al. (1995) used geometric shadow and linear mixture models to infer several important structural parameters of a boreal forest. Woodcock et al. (1994; 1997) estimated the mean tree size and cover for each forest stand through inversion of the Li-Strahler canopy reflectance model in Stanislaus National Forest and found the forest cover estimates more reliable. Gemmell (1999) tested the inversion of a geometric-optical forest reflectance model and the utility of two spectral indices (NDVI and SAVI) for estimating crown cover in a conifer forest site. Scarth and Phinn (2000) determined the forest crown cover projection, canopy size, tree densities and successional stage using an inverted geometric-optical model in mixed eucalypt forests in Australia. These studies used inversion of the geometric-optical model to monitor forest structural variables are all based on Landsat Thematic Mapper (TM) data. In addition, the authors also suggested that the development of new-generation imaging platforms would provide an opportunity to use multi-angular or hyperspectral remote sensing data for improving and calibrating the inversion of geometric-optical models. Therefore, the objective of this study is to evaluate the benefits of using EO-1 Hyperion hyperspectral data in combination with an inverted geometric-optical model for deriving and mapping two forest structural variables, crown closure (CC) and crown diameter (CD), in a broadleaved forest.

* Corresponding author.

2. STUDY AREA AND DATA COLLECTION

The study area, namely the Longmenhe forest nature reserve, lies in the Xingshan county of Hubei province, towards the northeast of Three Gorges Region in China (centred at 31°20′N, 110°29′E). The total reserve size is about 4’644 ha and the altitude varies around 1300 m above sea level. This study site belongs to the temperate climate zone (Cwa – Subtropical monsoon, Koeppen (McKnight and Hess, 2000)), average precipitation is about 100-150 mm per month and in spring-summer (April-September) season it can be as high as 200-300 mm per month. The Longmenhe forest reserve is mainly dominated by about 650 ha natural evergreen broadleaved forest and mixed deciduous broadleaved forest; 223 ha rare plant communities and 121 ha planted subtropical evergreen broadleaved forest.

Field data were collected in April to June of 2003. With support of 1:50,000 topographic maps, a total of 40 sample sites (100x100m) located in the study area were measured based on different plant strata and topographic distribution, and each of them randomly included 5 sample plots (20x20m), which provided relevant photos, plant profile and crown cover maps. Other measurements in each sample plot include the GPS locations and several important forest structural attributes, such as crown diameter and DBH from measuring tape; tree height and trunk height by altimeter; tree age using increment borer; and visual estimations by forest experts for forest type, plant species, crown closure and distribution.

For the study area, a Hyperion image was acquired on June 10, 2004, around 11:00 a.m. local time. Hyperion, one of the three sensors on the NASA EO-1 platform, was launched on November 2000 and orbited 1 min behind Landsat. As a pushbroom imaging instrument, Hyperion provides high resolution hyperspectral images capable of resolving 242 spectral bands (from 0.4–2.5 μm) with a 10 nm spectral resolution and a 30 m spatial resolution. Ancillary data also consisted of a digital elevation model (DEM) with 30 m spatial resolution, which is required for deriving the model inputs.

3. METHODS

The overall methods used in this study are shown as flowchart in Figure 1. The sequence involves:

1. Hyperion data processing, which includes effective band selection, de-striping, radiometric, atmospheric and geometric corrections;
2. Based on the at-surface reflectance data, deriving the per-pixel proportions of four scene components (sunlit canopy, sunlit background, shaded canopy and shaded background) by linear spectral unmixing analysis;
3. Using spectral angel mapping to classify the forest with support of field measurements and determine the relevant input parameters;
4. Inverting the Li-Strahler geometric-optical model integrated with pixel-based sunlit background fraction, canopy structural parameters, slope and aspect data to estimate crown closure and crown diameter;
5. Quantitatively assessing the accuracy of model retrievals through field data collected for 30 sample sites.

Therefore, the key of this study is the theory of the geometric-optical model.

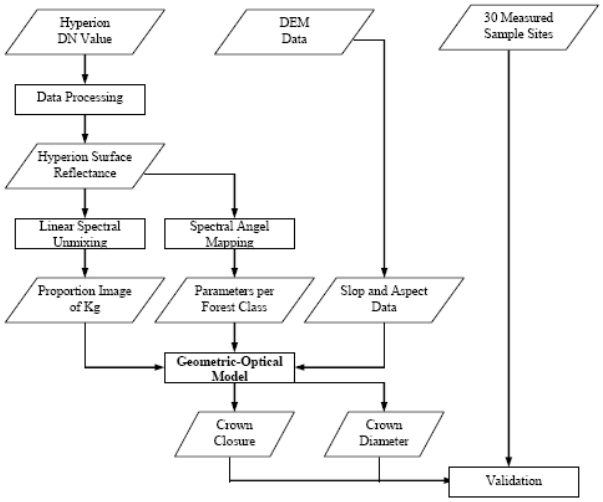

Figure 1. Flowchart of general methods

3.1 Geometric-Optical Model

The Li-Strahler geometric-optical model (Li and Strahler, 1992; 1985) was derived from the assumption that the Bidirectional Reflectance Distribution Function (BRDF) is a purely geometric phenomenon resulting from a scene of discrete three-dimensional objects being illuminated and viewed from different positions in the hemisphere. The reflectance associated with a given viewpoint is treated as an area-weighted sum of four fixed reflectance components: sunlit canopy, shaded canopy, sunlit background, and shaded background. Therefore, for each pixel of a remote sensing image the reflectance (S) can be modeled as a linear combination of four components (G, C, T, and Z: the reflectance of sunlit background, sunlit canopy, shaded canopy and shaded background respectively) and their areal proportions (Kg, Kc, Kt and Kz):

$$S = K_g G + K_c C + K_t T + K_z Z \quad (1)$$

The Li-Strahler model assumes that the resolution of the remote sensing image is much larger than the size of individual crowns but smaller than the size of forest stands, and that the individual trees are randomly (Poisson) distributed within the pixel (Woodcock et al., 1994). In this study, we use an ellipsoid model for the shape of a broadleaved forest tree crown. The relevant crown geometry parameters are tree height (h) from ground to mid-crown, crown radius (b) in vertical direction and crown radius (r) in horizontal direction. Based on the principle of three-dimensional geometry of an ellipsoid, each proportion of four components can be expressed by a combination of these structural parameters. For inverting the model, one component (sunlit background) can be used for deriving the expected forest variables: crown closure and crown diameter.

The proportion of sunlit background (Kg) can be formulated using the Boolean model (Strahler and Jupp, 1990):

$$K_g = e^{-\pi \cdot M \cdot [\sec(\theta_i) + \sec(\theta_v) - O(\theta_i, \theta_v, \phi)]} \quad (2)$$

Here, $O(\theta_i, \theta_v, \phi)$ is the average of the overlap function between illumination and viewing shadows of individual crowns as projected onto the background. ϕ is the difference in azimuth angle between illumination and viewing. θ_i, θ_v are the zenith

angles of illumination and viewing. M, called "treeness, is defined as $M=\Lambda R^2$, where Λ is the number of trees per unit area.

The exact solution for the overlap function on the principal plane can be determined as (Li and Strahler, 1992):

$$O(\theta_i,\theta_v,\phi)=1/\pi(\sec\ \theta_i''+\sec\ \theta_v'')(t-\sin t\ \cos t) \quad (3)$$

$$\cos t=\frac{h\left|\ \tan\theta_i''-\tan\theta_v''\cos\phi\ \right|}{b(\sec\theta_i''+\sec\theta_v'')} \quad (4)$$

Where t is valued in $[0,\ \pi/2]$. Therefore, in terms of equations (2) and (3), M can be inferred as:

$$M=\frac{-\ln(K_g)}{(\sec\theta_i''+\sec\theta_v'')(\pi-t+\cos t\ \sin t)} \quad (5)$$

In this study, for nadir viewed status, integrating the topographic effects, the illumination, viewing and slope angles corrected for the spheroidal shape of the crown are shown in equations (6)-(9) (Li and Wang, 1995; Schaaf et al., 1994):

$$\theta_i'=\arctan\left(\frac{\tan\theta_i}{r/b}\right) \quad (6)$$

$$\theta_s'=\frac{\pi}{2}-\arctan\left[\frac{\tan(\pi/2-\theta_s)}{r/b}\right] \quad (7)$$

$$\theta_i''=\arccos(\cos(\theta_i')\cos(\theta_s')+\sin(\theta_i')\sin(\theta_s')\cos(\varphi_i-\varphi_s)) \quad (8)$$

$$\theta_v''=\theta_s \quad (9)$$

Where (θ_s,φ_s) are the angles of slope and aspect.

Since M is an important parameter in the relationship between image variables and forest structure, in the case of Poisson distributed trees, the crown closure (CC) and crown diameter (CD=2xR) can be calculated as follows (Li and Strahler, 1985; Woodcock et al., 1997):

$$CC=1-e^{-\pi\cdot M} \quad (10)$$

$$R^2=\frac{\sqrt{(1+\omega)^2\cdot M^2+4\cdot V(m)\cdot\omega}-(1+\omega)\cdot M}{2\omega} \quad (11)$$

Where $V(m)$ is the variance of M, and ω is the coefficient of variation of the squared crown radius.

Consequently, according to equations (4)-(11) the necessary inverted model inputs for determining CC and CD are the proportional image of Kg; the solar zenith and azimuth angles (θ_i,φ_i); the view zenith and azimuth angles (θ_v,φ_v); the local slope and aspect (θ_s,φ_s) and the mean measured parameters for different kinds of forest crown shapes: r/b, h/b and ω.

3.2 Hyperion Data Processing

The currently used Hyperion Level 1B1 data have 242 bands of which 196 are nonzero and not overlapping. For converting DNs to radiances (W/m^2-sr-μm), the data were scaled by 40 for VNIR and 80 for SWIR (Radiance for VNIR=DN/40; Radiance for SWIR=DN/80) (Beck, 2003). Several stripes (data columns of poor quality) in the Hyperion data contain no information and lower radiance. Those abnormal pixels are detected and replaced by the average radiance value of their immediate left and right neighboring pixels (Han et al., 2002). The steps are comparing each pixel's value with its neighbors horizontally in each band, if the value is smaller than both neighbors this pixel is labelled as abnormal. Then the numbers of consecutive abnormal pixels is counted vertically, if the percentage of abnormal pixels in each column is greater than 55%, it will be treated as striping and be recalculated by the mean of their neighbors. In addition, a Minimum Noise Fraction (MNF) process can reduce the noise of a hyperspectral image (Green et al., 1988). Based on the Eigenvalue profile, the effective bands containing the most information are selected to obtain the final Hyperion data for model inversion.

Remote sensing data with accurate surface reflectance values are essential for a successful inversion of a canopy reflectance model. Thus, an atmospheric correction is required prior to data analysis. In this study, we use ACORN version 4.0, a commercially available atmospheric correction program based on the MODTRAN 4 radiative transfer code (AIG, 2002). ACORN uses two water absorption channels (940 and 1140nm) in Hyperion data to evaluate the amount of water vapor in combination with the visibility at the moment of data acquisition. Due to the low signal to noise ratio at the beginning and the end of the spectra ($\leq$436nm and $\geq$2385nm) and the heavy water absorption influences in several bands, a total of 64 bands are dropped from 196 valid bands. Geometric correction is done by 26 GCPs (Ground Control Points) relative to 1:50,000 topographic maps and the geometric error is less than one pixel. Finally, the corrected Hyperion data with 132 bands of surface reflectance in a UTM Zone 49 N WGS-84 projection are used in this study.

3.3 Linear Spectral Unmixing

Linear spectral unmixing has been widely used to calculate the percentages of several individual surface components contained in each pixel of a remote sensing image (Goodwin et al., 2005; Peddle et al., 1999). The method assumes that the reflectance (S) from each pixel is a linear combination of each endmember, which is the pure reflectance spectrum of a surface component. The general equations are

$$S_j=\sum_{i=1}^{m}K_iR_{i,j} \quad (12)$$

$$1=\sum_{i=1}^{m}K_i \quad (13)$$

Where m is the number of components; j is the bands and K is the fractional abundance of an endmember. In this study, on the basis of the Li-Strahler model, there are only four components (equation (1), G, C, T, and Z) contained in one pixel. Hence, the sum of the four proportions is equal to 1:

$$K_g+K_c+K_t+K_z=1 \quad (14)$$

Since the proportional image of Kg (sunlit background fraction) is required for inverting the model, selection of the suitable endmembers G, C, T, and Z is the most important issue. Usually, the endmembers are obtained from the observation of a field spectrometer, or are taken directly from a remote sensing image with sufficient field data, or from an existing spectral library. In this case, with the support of extensive in situ measurements, we select the four endmembers by trial and error from Hyperion training samples.

3.4 Spectral Angel Mapping

Spectral Angle Mapping (SAM) is one kind of algorithms for classifying hyperspectral data. In SAM, classification is carried out through comparing image spectra to individual endmembers. The similarity between an endmember and the per-pixel image spectrum is determined by calculating the "spectral angle", treating them as vectors in a space with a dimensionality equal to the number of bands. If the spectral angle between them is very small, it implies that the pixel is close to this endmember (Zeng, 2003).

SAM is used for forest classification in the Longmenhe study area for determining the required model inputs of the pixel-based forest crown shape parameters. Thanks to every homogeneous forest region is much more than one pixel of 30 m, 7 endmembers representing the different dominant forest communities and species are detected directly from Hyperion data based on the field measurements. For each pixel, the spectral angles comparing with each endmember are calculated and then the pixel will be assigned to the class of endmember with the smallest angle. We use a standard angle threshold of 0.1 radians to identify unclassified pixels. The accuracy of SAM classification is estimated by a confusion matrix based on 40 independent field sample sites.

4. RESULTS

4.1 Model Input Data

The processed Hyperion data with surface reflectance is shown in Figure 2a. Because of the cloud cover affecting the quality of this image, finally we use an image subset of size 208 (column) x 173 (line) x132 (band). After analyzing and comparing the training samples collected from the fieldwork, such as a small playground of a primary school, a bare farming place, closed and open forest regions, etc., the purest pixels representing the endmembers of four components, sunlit background G, sunlit canopy C, shaded canopy T and shaded background Z, are selected from the Hyperion image (Figure 3). Combined with equation (1) and (14), the areal proportions of Kg, Kc, Kt and Kz are calculated for each pixel, and the proportional image of Kg is shown in Figure 2b. The brighter regions express higher proportions. Here, we assume $0 \leq Kg \leq 1$, although a few pixels in the linear spectral unmixing approach produced negative fractions, which subsequently are recoded as infeasible areas. Most of these pixels are located in the topographic shadow of the sloped terrain.

As mentioned at the end of section 3.1, besides the proportion Kg, the other required inputs for inversion of the Li-Strahler model, slope and aspect images are derived from DEM data using topographic analysis model of ERDAS IMAGINE, see Figure 2c-d. In addition, this nadir viewed Hyperion image was acquired at a 23.55°solar zenith and 104.50°solar azimuth angle.

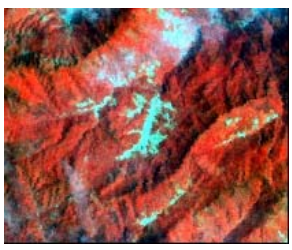

a. Hyperion image (bands-R: 50 G: 23 B: 16)

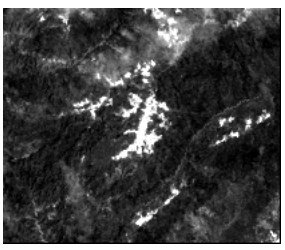

b. Proportional image of Kg

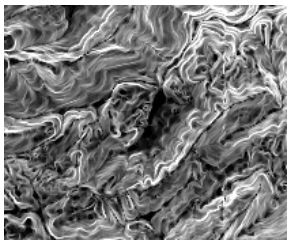

c. Slope data with 30m resolution

d. Aspect data with 30m resolution

Figure 2: Processed Hyperion data and necessary inputs for inversion of the Li-Strahler model

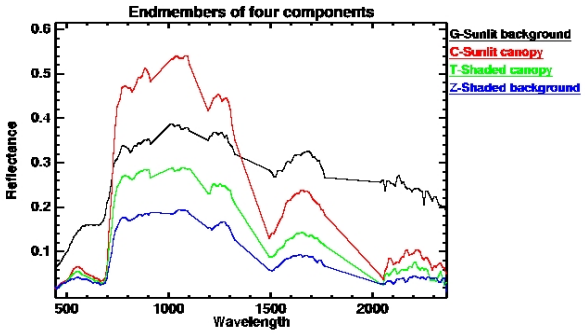

Figure 3: Four Endmembers derived from the Hyperion image (G-sunlit background; C-sunlit canopy; T-shaded canopy and Z-shaded background)

4.2 Forest Classification

In this study area, the dominant forest communities include deciduous broadleaved forest, evergreen broadleaved forest, and conifer forest. Most of the collected field sample sites (100x100m) were chosen in a homogeneous forest with different predominant species. Finally, 7 pixels indicating the typical forest classes' spectra as endmembers are detected from the Hyperion image. Those are 1. Deciduous broadleaved forest (*Platacarya strobilacea*); 2. Deciduous broadleaved forest (*Quercus glandulifera var. brevipetiolata*); 3. Deciduous broadleaved forest (*Betula luminifera*); 4. Evergreen broadleaved forest (*Quercus spinosa*); 5. Evergreen broadleaved forest (*Cyclobalanopsis oxyodon*); 6. Coniferous forest (*Pinus tabulaeformis tabulaeformis*); and 7. Coniferous forest (*Larix keaempferi*). We separately recode the deciduous broadleaved forest, evergreen broadleaved forest, and conifer forest into class 1, 2 and 3, respectively. We consider class 0 as being unclassified pixels, when a SAM distance of more than 0.1 radians has been calculated comparing to the remaining other 7 endmembers. Class 0 includes both the non-forested regions as well as regions that were affected by clouds or shadows.

Field measurements (40 samples)	SAM classes			Total	Accuracy
	DB	EB	C		
Deciduous Broadleaved Forest	17	3	1	21	81%
Evergreen Broadleaved Forest	2	8	0	10	80%
Conifer Forest	2	1	6	9	67%
Total	21	12	7	31/40	**78%**

Table 1. Confusion matrix of the SAM classification result

Using 40 field sample sites to validate the SAM forest classification result, the confusion matrix (Table 1) indicates that the percentage of correct classification reaches 78%. In terms of the field measurements, the corresponding mean value of forest crown parameters, h, b, r and ω for every dominant forest class is shown in Table 2.

Dominant Forests	h	b	r	w
Deciduous Broadleaved Forest	9.79	3.97	1.79	1.25
Evergreen Broadleaved Forest	8.86	3.36	1.61	3.02
Conifer Forest	8.41	4.63	1.51	1.87

Table 2. Inverted model inputs for each forest class

4.3 Model Output and Validation

We design and compile an IDL program to implement the inversion of the Li-Strahler model integrated with the pixel-based input data. Figure 4 presents the final mapping results of forest structural variables, crown closure and crown diameter, distributed in the Longmenhe study area.

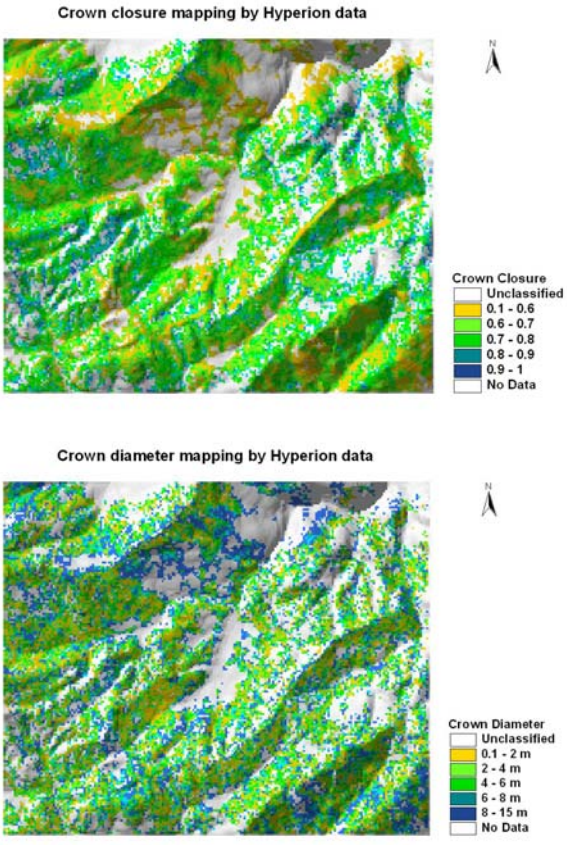

Figure 4. Mapping results of forest crown closure and crown diameter by the inverted geometric-optical model

For validating the model outputs, we use the mean value of a 3x3 window for comparison to one field sample site. Figure 5 illustrates the agreement between model-interpreted CC/CD and ground-measured values. In total 30 independent samples are included. The closer the points to the 1:1 line, the better the predicted results are. The coefficient of determination R^2 is equal to 0.64 for CC and 0.54 for CD. The calculated root mean squared error is $RMSE_{CC}$= 0.058 and $RMSE_{CD}$= 0.71. Although most of the interpreted results of CC seem to be less than the field measured values as well as the values of CD partly do not match the ground data very well, the reliability of model output is considered to be acceptable.

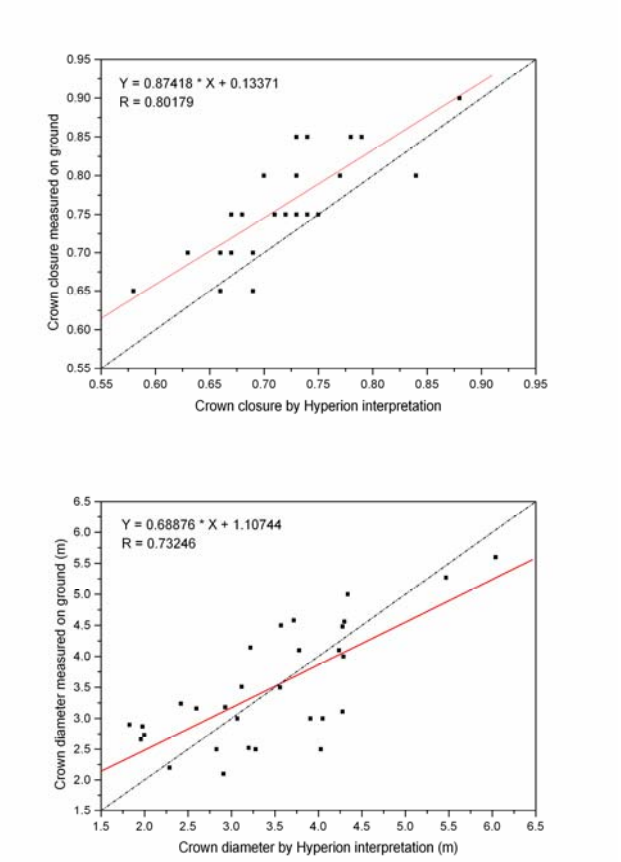

Figure 5. Linear relationship between ground measured CC/CD and model derived CC/CD

5. CONCLUSION AND OUTLOOK

The inverted geometric-optical model combined with the spectral unmixing analysis used in this study proved to be useful to derive forest canopy structural variables from Hyperion data in the Longmenhe broadleaved forest. The accuracy of the inverted model results mainly depends on the detectability of M ('treeness'). Thus, as shown in equation (5), for a better calibration of the model, a sensitivity analysis may be performed, estimating the sensitivity of M to the sunlit background fraction (Kg), the crown shape parameters r/b, h/b and the calculated slope/aspect angles.

The accuracy of both, the forest classification and the field measurements are substantially influencing the model input parameters. Several methods using hyperspectral data based classification approaches have been documented in literature, and this contribution positions itself well in the generally achieved classification accuracies. However, choosing 30 sample sites for validating the model results has been found to be at the lower limit to achieve successful model accuracies. We will in the future investigate, if high spatial resolution data can increase the model accuracy by combining these two approaches.

We evaluated the use of spaceborne imaging spectrometer data in combination with a physical- based canopy reflectance model to determine forest structural variables at regional scale to be

efficient and useful. Even though selected procedures will need more careful analysis in the future, the presented results show confidence in the approach selected. Besides the crown closure and crown diameter variables, other forest structural and biophysical attributes, like stem density, tree height, DBH, age and LAI, can also possibly be estimated more exactly by the inversion of canopy reflectance models with support of high spatial and hyperspectral remote sensing data. Consequently, quantitative monitoring the forest ecosystem and its changes over time using effective and coherent models will be a major future goal.

ACKNOWLEDGMENT

We gratefully acknowledge financial support from the 'Knowledge Innovation Project' of the Chinese Academy of Sciences (No. KZCX3-SW-334). We appreciate support from Xu Wenting, Huang Jianxi and Tian Yichen for participation in the field campaign.

REFERENCES

AIG, 2002. ACORN 4.0 User's Guide, Boulder, CO: Analytical Imaging and Geophysics LLC.

Beck, R., 2003. EO-1 User Guide - Version 2.3, Satellite Systems Branch, USGS Earth Resources Observation Systems Data Center (EDC).

Gemmell, F., 1999. Estimating conifer forest cover with thematic mapper data using reflectance model inversions and two spectral indices in a site with variable background characteristics. *Remote Sensing of Environment*, 69(2): 105-121.

GLP, 2005. Science Plan and Implenetation Strategy. IGBP Report No. 53/IHDP Report No. 19. Stockholm.

Goodwin, N., Coops, N.C. and Stone, C., 2005. Assessing plantation canopy condition from airborne imagery using spectral mixture analysis and fractional abundances. *International Journal of Applied Earth Observation and Geoinformation*, 7(1): 11-28.

Green, A.A., Berman, M., Switzer, P. and Craig, M.D., 1988. A Transformation for Ordering Multispectral Data in Terms of Image Quality with Implications for Noise Removal. *IEEE Transactions on Geoscience and Remote Sensing*, 26(1): 65-74.

Hall, F.G., Shimabukuro, Y.E. and Huemmrich, K.F., 1995. Remote-Sensing of Forest Biophysical Structure Using Mixture Decomposition and Geometric Reflectance Models. *Ecological Applications*, 5(4): 993-1013.

Han, T., Goodenough, D.G., Dyk, A. and Love, J., 2002. Detection and correction of abnormal pixels in hyperion images. *International Geoscience and Remote Sensing Symposium (IGARSS)*, pp. 1327-1330.

Li, X. and Strahler, A., 1992. Geometric-optical bidirectional reflectance modeling of the discrete crown vegetation canopy: Effect of crown shape and mutual shadowing. *IEEE Transactions on Geoscience and Remote Sensing*, 30: 276-292.

Li, X. and Strahler, A.H., 1985. Geometric-optical modeling of a conifer forest canopy. *IEEE Transactions on Geoscience and Remote Sensing*, GE-23(5): 705-721.

Li, X. and Wang, J., 1995. *Vegetation Optical Remote Sensing Models and Vegetation Structure Parameterization*. Science Press, Beijing, 118 pp.

Liang, S., 2004. *Quantitative remote sensing of land surfaces*. Wiley series in remote sensing. Wiley-Interscience, Hoboken, NJ, XXVI, 534 pp.

McKnight, T.L. and Hess, D., 2000. Climate Zones and Types: Dry Humid Subtropical Climate (Cfa, Cwa). Physical Geography: A Landscape Appreciation. Upper Saddle River, NJ: Prentice Hall, 223-6 pp.

Murai, S., 1991. *Applications of remote sensing in Asia and Oceania-Environmental change monitoring*. Asian association on remote sensing, Tokyo.

Peddle, D.R., Hall, F.G. and LeDrew, E.F., 1999. Spectral Mixture Analysis and Geometric-Optical Reflectance Modeling of Boreal Forest Biophysical Structure. *Remote Sensing of Environment*, 67(3): 288-297.

Scarth, P. and Phinn, S., 2000. Determining Forest Structural Attributes Using an Inverted Geometric-Optical Model in Mixed Eucalypt Forests, Southeast Queensland, Australia. *Remote Sensing of Environment*, 71(2): 141-157.

Schaaf, C.B., Li, X.W. and Strahler, A.H., 1994. Topographic Effects on Bidirectional and Hemispherical Reflectances Calculated with a Geometric-Optical Canopy Model. *IEEE Transactions on Geoscience and Remote Sensing*, 32(6): 1186-1193.

Schimel, D.S., House, J.I., Hibbard, K.A., Bousquet, P., Ciais, P., Peylin, P., Braswell, B.H., Apps, M.J., Baker, D., Bondeau, A., Canadell, J., Churkina, G., Cramer, W., Denning, A.S., Field, C.B., Friedlingstein, P., Goodale, C., Heimann, M., Houghton, R.A., Melillo, J.M., Moore, B., Murdiyarso, D., Noble, I., Pacala, S.W., Prentice, I.C., Raupach, M.R., Rayner, P.J., Scholes, R.J., Steffen, W.L. and Wirth, C., 2001. Recent patterns and mechanisms of carbon exchange by terrestrial ecosystems. *Nature*, 414(6860): 169-172.

Strahler, A.H. and Jupp, D.L.B., 1990. Modeling Bidirectional Reflectance of Forests and Woodlands Using Boolean Models and Geometric Optics. *Remote Sensing of Environment*, 34(3): 153-166.

Ustin, S.L., 2004. *Remote sensing for natural resource management and environmental monitoring*. Wiley, Hoboken, NJ, XXXII, 736 pp.

Woodcock, C.E., 1994. Estimation of forest stand structure from Landsat TM through inversion of the Li-Strahler model. *International Geoscience and Remote Sensing Symposium (IGARSS)*, pp. 1245-1247.

Woodcock, C.E., Collins, J.B., Gopal, S., Jakabhazy, V.D., Li, X., Macomber, S., Ryherd, S., Judson Harward, V., Levitan, J., Wu, Y. and Warbington, R., 1994.

Mapping forest vegetation using Landsat TM imagery and a canopy reflectance model. *Remote Sensing of Environment*, 50(3): 240-254.

Woodcock, C.E., Collins, J.B., Jakabhazy, V.D., Li, X., Macomber, S.A. and Wu, Y., 1997. Inversion of the Li-Strahler canopy reflectance model for mapping forest structure. *IEEE Transactions on Geoscience and Remote Sensing*, 35(2): 405-414.

Wulder, M., 1998. Optical remote-sensing techniques for the assessment of forest inventory and biophysical parameters. *Progress in Physical Geography*, 22(4): 449-476.

Zeng, Y., 2003. Using hyperspectral data for identifying geological and soil units in the Alora region, Southern Spain. Thesis report, Centre for Geo-information, Wageningen University and Research Centre, GIRS-2003-23, 57 pp.